

PAPER • OPEN ACCESS

## Studies on mechanical property of squeeze cast and heat treated AA6061-ZrO<sub>2</sub> composite

To cite this article: A Raja Annamalai *et al* 2020 *Mater. Res. Express* 7 086506

View the [article online](#) for updates and enhancements.



The Electrochemical Society  
Advancing solid state & electrochemical science & technology  
2021 Virtual Education

**Fundamentals of Electrochemistry:**  
Basic Theory and Kinetic Methods  
Instructed by: **Dr. James Noël**  
Sun, Sept 19 & Mon, Sept 20 at 12h–15h ET

Register early and save!



# Materials Research Express



## PAPER

# Studies on mechanical property of squeeze cast and heat treated AA6061-ZrO<sub>2</sub> composite

### OPEN ACCESS

#### RECEIVED

23 June 2020

#### REVISED

22 July 2020

#### ACCEPTED FOR PUBLICATION

30 July 2020

#### PUBLISHED

7 August 2020

Original content from this work may be used under the terms of the [Creative Commons Attribution 4.0 licence](#).

Any further distribution of this work must maintain attribution to the author(s) and the title of the work, journal citation and DOI.



A Raja Annamalai<sup>1</sup>, Johny James<sup>2</sup> , P Kuppan<sup>3</sup>, S Hemakumar<sup>3</sup> and Chun-Ping Jen<sup>4,5</sup> 

<sup>1</sup> Centre for Innovative Manufacturing Research, VIT, Vellore- 632014, India

<sup>2</sup> Sri Venkateswara College of Engineering & Technology, Chittoor- 517127, India

<sup>3</sup> School of Mechanical Engineering, VIT, Vellore- 632014, India

<sup>4</sup> Department of Mechanical Engineering, National Chung Cheng University, Chia-Yi, Taiwan

<sup>5</sup> Author to whom any correspondence should be addressed.

E-mail: [Raja.annamalai@vit.ac.in](mailto:Raja.annamalai@vit.ac.in), [johnyjames2002@yahoo.com](mailto:johnyjames2002@yahoo.com), [pkuppan@vit.ac.in](mailto:pkuppan@vit.ac.in), [mail2hemakumar@gmail.com](mailto:mail2hemakumar@gmail.com) and [imecjp@ccu.edu.edu.tw](mailto:imecjp@ccu.edu.edu.tw)

**Keywords:** AA6061, aging, hardness, tensile, ZrO<sub>2</sub>

## Abstract

This work deals with processing, characterization, and study of the mechanical property of AA6061-ZrO<sub>2</sub> composite by stir casting unit combined with squeeze casting setup. Morphology study of the refined composite was measured with the help of Optical Microscope and Scanning Electron Microscopy (SEM). The Energy Dispersive x-ray spectroscopy was performed to observe the desirable elements present in the processed composite. The EDX investigation endorses the presence of Aluminum, Zirconium, and Oxygen, are the elements of the desirability. The processed composite displayed increased hardness value when related to the base aluminum alloy AA6061 at test conditions. The tensile tests have been performed for the refined specimen both in cast and heat treated conditions. 20%–63% improvement in tensile strength as an outcome of the inclusion of ZrO<sub>2</sub> particles and heat treatment process was recorded, and the fashion was analyzed. Finally, all the three composite specimens were tested for wear resistance property for the support of pin on disc wear test kit. The wear trend due to the addition of ZrO<sub>2</sub> particles was discussed in a detailed manner.

## Introduction

The density of aluminum is lesser when related to copper and Titanium. This identifies aluminum is the best for low weight applications, particularly in aerospace; automotive and marine, etc [1–5]. Also aluminum can be simply melted down and recycled 100%, this characteristic of low melting point related to steel, and Iron makes aluminum environmental-friendly and excellent material. Applications such as aerospace, automotive and structural require high strength. The compressive strength, hardness, and toughness can be improved by the insertion of reinforcement material [6]. Though magnesium is low-density metal it has its own demerits. Adding reinforcement to the matrix phase is the concept of the composite. It is a well-known fact that when related to fibre or whisker, particle reinforcement has a number of advantages. This particle reinforced composite have replaced Iron and steel materials [7]. There are various reinforcements like SiC, TiB<sub>2</sub>, B<sub>4</sub>C, TiC, ZrSiO<sub>4</sub>, Al<sub>2</sub>O<sub>3</sub>, WC and TiO<sub>2</sub> are included within the metal matrix for various applications [8]. But ZrO<sub>2</sub> offers a large number of greater properties like very high resistance to crack formation and propagation, high fracture toughness value, i.e. 10 MPa.m<sup>1/2</sup> and wear resistance, etc as shown in table 1. Singh J, Chauhan A (2019) made a review on the properties and wear behavior of hybrid aluminium matrix composites fabricated via stir casting route [9]. Fairouz *et al* (2017) Combined 6061 Al alloy with 5 vol% SiC with a size of 8 μm and prepared successfully to use stir casting method followed by squeeze casting technique [10]. Kannan *et al* (2018) studied the performance of both aluminum alloy AA 7075 and hybrid nanocomposite material of AA 7075 reinforced with BN and Al<sub>2</sub>O<sub>3</sub> nanoparticles by employing squeeze casting rig [11]. Composite is mainly used to produce automotive as well as aerospace components where wear is a prime function [12, 13]. The inclusion of ceramic particles enhances the

**Table 1.** Property of Metal Matrix AA 6061 and Zirconium Oxide (ZrO<sub>2</sub>).

Metal Matrix AA 6061		Zirconium Oxide (ZrO <sub>2</sub> )	
Density	2.7 g cm <sup>-3</sup>	Chemical formula	ZrO <sub>2</sub>
Melting Point	582 °C–652 °C	Molar mass	123.218 g mol <sup>-1</sup>
Brinell Hardness	30–33	Appearance	White Powder
Hardness, Vickers	107	Density	5.68 g cm <sup>-3</sup>
Ultimate Tensile Strength	110 MPa	Melting point	2715 °C
Fatigue Strength	96.5 MPa	Compressive Strength	1200–5200 MPa
Machinability	50%	Hardness, Vickers	1220
Solution Temperature	529 °C	Tensile Strength	115–711 MPa

strength of the parent material [14]. Many researchers proved this process of enhancing strength [15]. In addition to that mechanical property can be enhanced by solution heat treatment and aging process. It is always essential to realize the function of the particle reinforcements and in which manner they impact precipitation process. In the aging process, metastable Mg<sub>2</sub>Si precipitates are created, which is associated with the mechanical property of AA 6061 alloy [16]. Chen and Lin studied the aging behavior of AA 6061 composite reinforced with TiC and Y<sub>2</sub>O<sub>3</sub>. The result shows an enhancement of about 66% hardness after solution treatment [17]. Even though there are few works related to the aging performance of aluminum composite, aging performance of Al 6061-ZrO<sub>2</sub> composite's work of literature is not available. Karthikeyan *et al* fashioned a composite with LM6 as matrix and ZrO<sub>2</sub> particles as reinforcement by stir casting rig. The machined samples were tested for wear resistant behavior at diverse loads by pin-on-disc wear experiment facility. He investigated and stated that the rate of wear of LM6 decreases with the rise in ZrO<sub>2</sub> particle content. Similarly, the coefficient of friction of LM25 alloy drops with the escalation in ZrO<sub>2</sub> [18]. Kumar *et al* produced a hybrid metal matrix composite with the help of Al-Si-Mg, Zircon, and alumina using stir casting. The wear-resistant characteristic of the produced composite material was examined using wear testing equipment. It was identified from the results that the composites having 3.75% ZrSiO<sub>4</sub> + 11.25% Al<sub>2</sub>O<sub>3</sub> has superior wear resistance property [19]. Pradhan *et al* investigated wear behavior of aluminum composites and friction with the help of SiC particles at diverse environments. The investigations were accomplished using the pin-on-disc tribo tester. The produced composite sample glides upon a disc made up of alumina at variable sliding speed and normal load. It was noticed that wear resistant property was in a straight line related to loading and sliding speed. Furthermore, the applied normal load and friction coefficient were inversely proportional [20].

This research work makes an effort to design and produce AA 6061-ZrO<sub>2</sub> composite with the help of modified to stir casting process coupled with squeeze casting to overcome the failures which occurs in gravity casting. Notwithstanding there are many kinds of reinforcement in the composite manufacturing industry this work introduces ZrO<sub>2</sub> in varying composition. In addition to that, the trend of hardness value and tensile value is because of the addition of ZrO<sub>2</sub> particles are recorded in detail. The cast composite was subjected to the heat treatment to enhance its mechanical property. The solution treatment was performed to develop the homogenization of ZrO<sub>2</sub> particles in the AA6061 matrix of the cast composite. Furthermore, wear is an important property of needs to be enhanced to increase the performance and life of moving components, especially in auto motives. The enhancement of wear resistance property and wear trend was discussed in detail. These research results and analysis take the developed material a substitute for conventional material, especially in aerospace, automotive and in defense industries in order to manufacture brake drum, Bicycle frames, engine cylinder surfaces and rotating blades of helicopters.

## Materials and methods

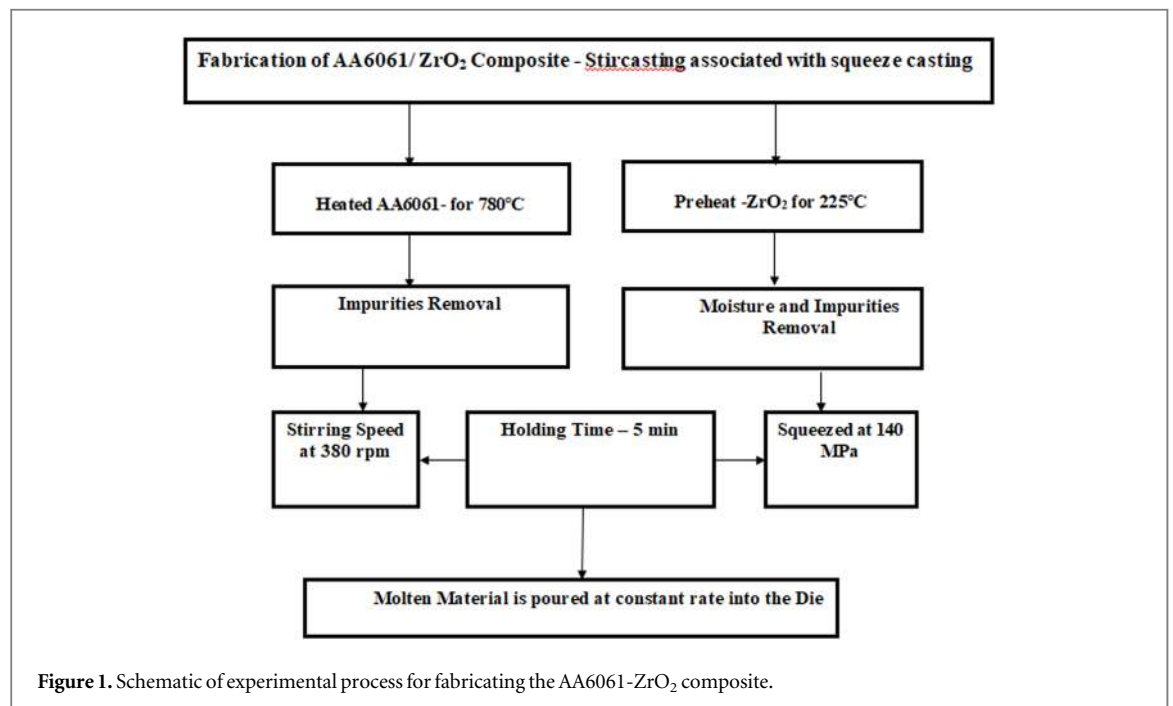
The elements required to process aluminum metal matrix composite were designed judicially in lined with the industry requirement. AA 6061 aluminum alloy was chosen as the metal matrix since it widely replaces iron and steel because of low weight and other distinctive properties as displayed in table 1 [21]. Also the chemical compositions of AA 6061 in percentage are presented in table 2. ZrO<sub>2</sub> particle reinforcement was chosen due to its availability and weird properties. The shape of ZrO<sub>2</sub> particle used was irregular, and the mean size of the reinforcement particles was 20 micrometers, and the same can be acknowledged with the help of the SEM image as shown in figure 3(b). The composition percentage was discreetly designed from 0–15 weight percent to achieve optimal property as tabularized in table 3. The processing technique carefully chosen was stir-casting associated with squeeze casting unit, which controls pores during solidification. Schematic representation of the experimental process for fabricating the AA6061-ZrO<sub>2</sub> composite is presented in figure 1. The metal matrix AA 6061 was melted in a Steel crucible by increasing the temperature of the electric furnace up to 780 °C. The ZrO<sub>2</sub>

**Table 2.** Chemical Compositions of AA 6061 in Percentage.

AA 6061	Mg	Si	Ti	Mn	Cr	Fe	Cu	Zn	Al	Others
%	0.8–1.2	0.40–0.80	Max 0.15	Max 0.15	0.04–0.35	Max 0.70	0.15–0.40	Max 0.25	Balance	0.05

**Table 3.** Composition and weight percent details of processed alloy and cast composite.

Specimen no	Composition	wt % of ZrO <sub>2</sub>	AA6061
1	AA6061	0	Remaining
2	AA6061-5 ZrO <sub>2</sub>	5	Remaining
3	AA6061-10 ZrO <sub>2</sub>	10	Remaining
4	AA6061-15 ZrO <sub>2</sub>	15	Remaining

**Figure 1.** Schematic of experimental process for fabricating the AA6061-ZrO<sub>2</sub> composite.

reinforcement particles were preheated up to 225 °C simultaneously in another furnace. As soon as the aluminum becomes molten metal 1.5 g (For 2 kg AA6061) of Magnesium was added to enhance its wettability property between both matrix and reinforcement phase [22]. Also, before inserting reinforcement particles into the molten alloy, the mixture was stirred at a speed of 380 rpm. The impurities formed at the top of the melt as a layer was removed. While stirring 10 g of coverall (a mixture of Potassium chloride + Nitric acid) of 5 gm per kg was added to the melt. This produces a thin film of the layer on top of the melt and thus avoids contacting of molten metal from the atmosphere. While continuously stirring the melt a vortex was made, right at the vortex, the preheated ZrO<sub>2</sub> reinforcement particles were decanted so that both reinforcement and matrix phase get mixed systematically. The properly mixed composite melt was decanted into the steel (H13 die steel) die having 50 mm diameter and 300 mm length and squeezed at 140 MPa pressure. The processed composite casting was machined to craft test samples as exhibited in figure 2. Theoretical density was derived using the rule of mixtures, and the actual density was calculated using Archimedes' Principle. The characterization was carried out using optical and SEM images. The cast composite specimens were solid solution treated at 590 °C in a furnace for one hour and quenched in water at normal room temperature. The solution treated samples were aged at 205 °C for six hours and cooled naturally. The hardness of the developed composite specimens carved as per ASTM E384 standard was investigated using Vickers Micro hardness tester ranges from 10–1000 gf before and after the heat treatment. The tensile specimens both as-cast and as heat treated was crafted from the cast composites from the middle of the rod and incised as per ASTM B557 standard (A—Length of reduced parallel section, min—36 mm, D—Diameter-6 mm, G—Gauge length- 30 mm) with the help of wire cut Electrical Discharge Machining to the required dimensions. Servo-hydraulic universal testing machine, Model: Instron 8801 was

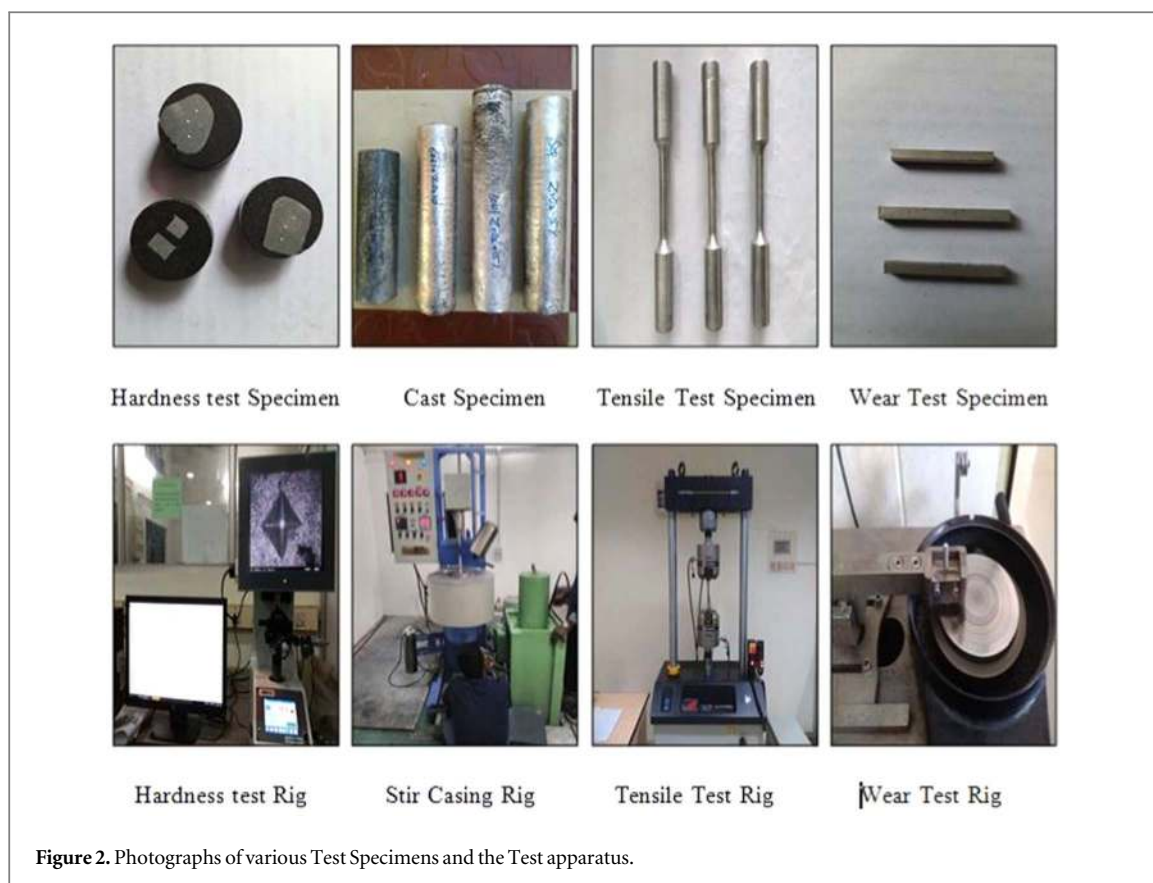


Figure 2. Photographs of various Test Specimens and the Test apparatus.

employed to test the tensile specimens. The failure analysis of fractured specimens was analyzed with the help of SEM images. Finally, the processed composites were tested for wear property with the help of Pin-on-Disc wear and friction testing Ducom equipment -TR 201 LE.

## Results and discussion

### Characterization of synthesized composite material

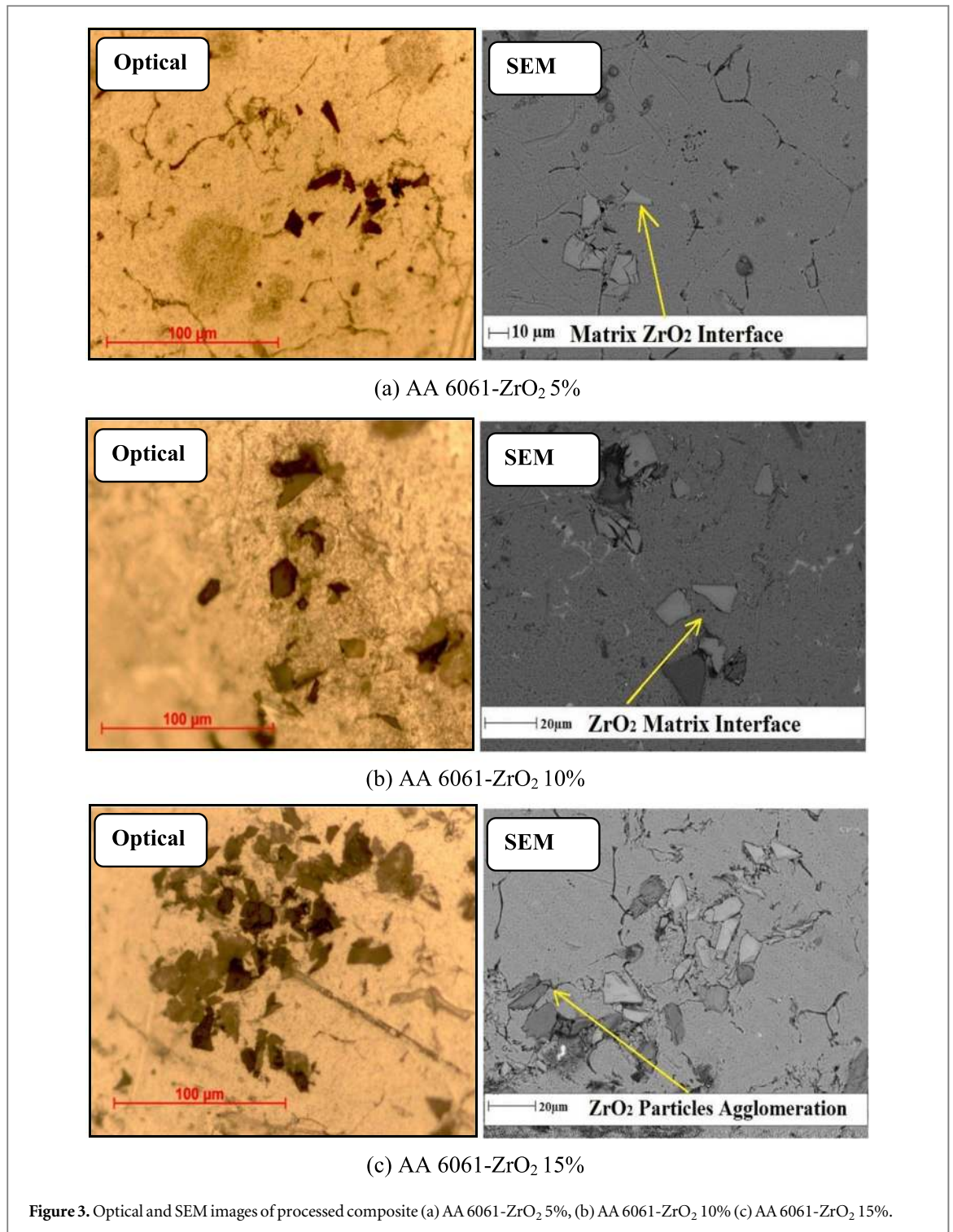
In order to make sure the presence and behavior of  $ZrO_2$  reinforcement particles in the AA6061 metal matrix, samples for microstructural examination were prepared from cast composites. Both optical and SEM images were captured and shown in figure 3. The captured images of AA6061- $ZrO_2$  5, 10 and 15% composites reveal the presence of  $ZrO_2$  reinforcement particles in the metal matrix. Furthermore, some agglomerations of reinforcement particles are realized in optical images, especially in AA6061- $ZrO_2$  15% sample as shown in figure 3(c) this ascribes is because of the inappropriate scattering and mixing of particle reinforcements in the metal phase. This agglomerate will drop amid the machining procedure as the metal matrix fails to catch hold of the reinforcement particles. This creates the mode for pores in the cast composite. SEM pictures clearly demonstrate the size and form of  $ZrO_2$  particles and with the assistance of showed the scale in the images, the sizes of the particles are evidently estimated, and it is an average of 20 micrometers.

### Porosity and density of processed AA 6061 and AA 6061- $ZrO_2$ composite

Table 4 presents the quantitative wt% of porosity. The cast AA 6061 alloy and composites are acceptable on the level of porosity is within the limit, i.e. less than 7%. The  $ZrO_2$  particle utilized as reinforcement in the processing of composite has a density value of  $5.68 \text{ g cm}^{-3}$ . Due to the higher density of the reinforcement over the parent alloy combination, the hypothetical density of the composite was found to increment in extent with wt% of reinforcements as presented in table 4.

The experimental density of all developed composites was found to pursue the pattern of theoretical density, which showed the fruitful manufacture of these composites through stir and squeeze casting methods. The composite strengthened with 15 weights per cent,  $ZrO_2$  was found to have the most elevated density among all sample specimens. This may be credited with high-density  $ZrO_2$  particles.

It was visible that porosity of AA 6061- $ZrO_2$  5% composite was lower than the unreinforced alloy. This credit is because of the constrained weight percent composition of  $ZrO_2$  particles, and because of the way that



the plastic working instigates the pore shutting. Additionally, it was discovered that the porosity of AA 6061-ZrO<sub>2</sub> 10% and AA 6061-ZrO<sub>2</sub> 15% composite was higher than the parent material AA 6061. This may have been related to issues, for example, poor wettability attributes, clustering, particle agglomeration and pore nucleation at the interface with deficient mechanical mixing. By and large, the agglomeration of reinforcement and resulting clustering gives a block to the fluid metal stream. The preheating of reinforcement could decrease the wettability issues forced by particles and prompt better dispersion in the liquid metal. The percentage porosity was ascertained for all composites and parent alloy using the formula as mentioned below in equation (1).

$$\% \text{ of porosity} = (\text{Theoretical density} - \text{Experimental density} / \text{Theoretical density}) \times 100 \quad (1)$$

The porosity in the metal matrix composites is initiated because of the ill-advised interfacial response between the ceramic reinforcements and the matrix. This interfacial response is primarily affected by the elements, for

**Table 4.** Density and Porosity of AA 6061 and AA 6061-ZrO<sub>2</sub> Composite.

Cast materials (wt%)	Density, g cm <sup>-3</sup>		Porosity (%)
	Experimental	Theoretical	
AA 6061	2.54	2.70	5.78
AA 6061-ZrO <sub>2</sub> 5%	2.69	2.84	5.27
AA 6061-ZrO <sub>2</sub> 10%	2.79	2.99	6.30
AA 6061-ZrO <sub>2</sub> 15%	2.94	3.14	6.30

example, convection properties, free energy at the interface, and temperature gradient that exists among particles and matrix during solidification notwithstanding different parameters viz. mixing speed, clustering, melt viscosity, the density difference between melt and particles.

### The weight percent of elements in the processed composite

The newly designed and refined composite was studied with the help of EDX Spectroscopy to see and analyze the presence of total elements in the processed composite. EDX Spectroscopy detected a list of elements present in the processed composite and its weight percent as displayed in figures 4(a) and (b) displays the mapping of elements of attraction in this research, i.e. Zirconium, Aluminum and oxygen.

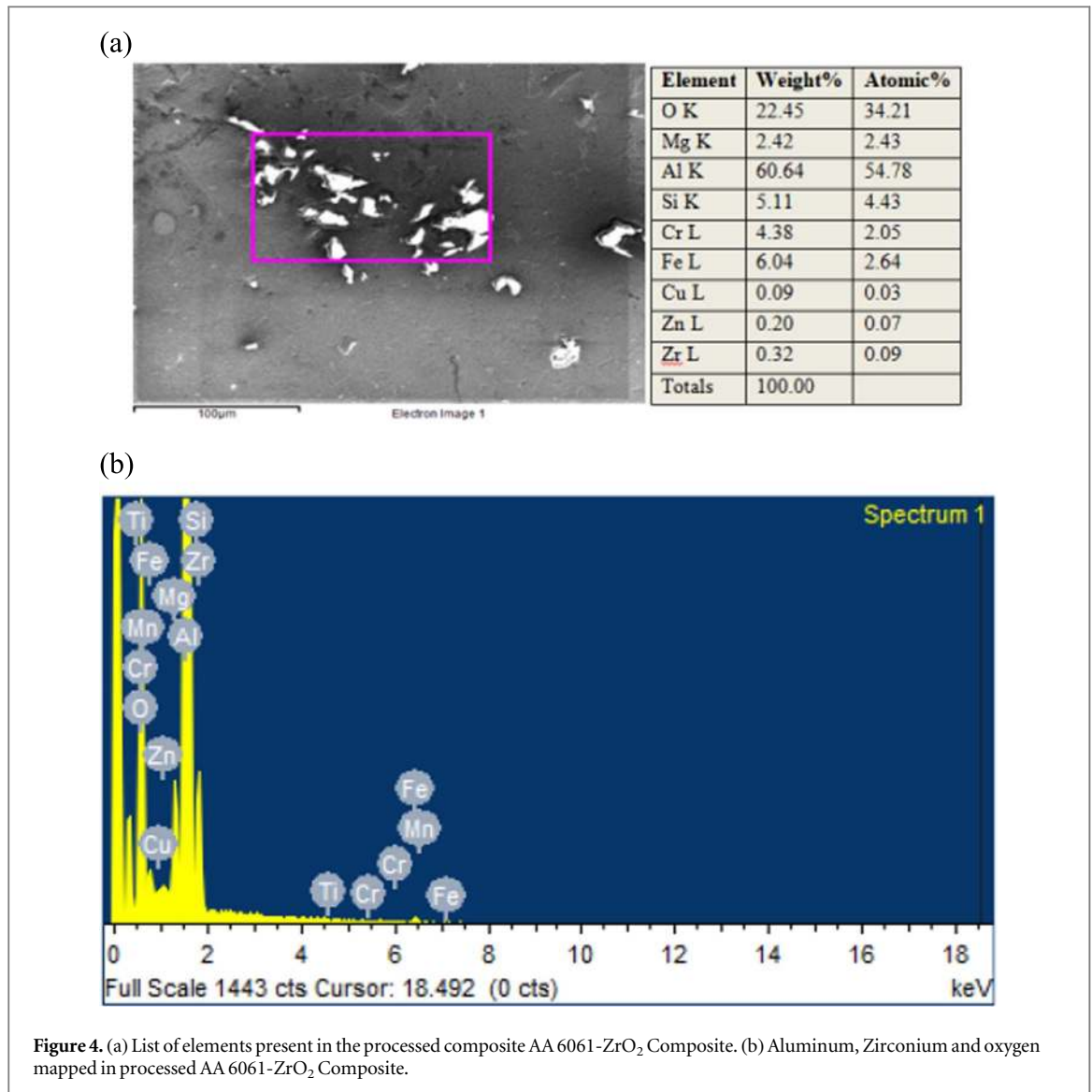
### X-ray diffraction of processed AA 6061-ZrO<sub>2</sub> composites before and after heat treatment process

The x-ray diffraction arrangements of the AA 6061 alloy and processed AA 6061-ZrO<sub>2</sub> composites taken place during processing as well as heat treatment is presented in figures 5(a) and (b). The pattern discovered the major peak of aluminum (PDF- 85-137) in all the seven samples. Figures 5(a) and (b) confirms the presence of traces of ZrO<sub>2</sub> (PDF- 89-9069) in the entire AA 6061-ZrO<sub>2</sub> composite sample but not in an AA 6061 sample. Figure 5(a) validates no interaction of ZrO<sub>2</sub> particles and AA 6061 as this x-ray diffraction shows no other considerable peaks. When the x-ray diffraction of heat treated AA 6061-ZrO<sub>2</sub> composite samples were acutely analysed as shown in figure 5(b) apart from AA 6061 and ZrO<sub>2</sub> peaks Mg<sub>2</sub>Si (PDF-75-0455) peaks were detected. These Mg<sub>2</sub>Si precipitates were identified in optical microscopy, and the formation of the same reflected in the enhancement of tensile strength. The diffraction arrangements were recognized by association with standard ASTM cards.

### Impact of aging on Hardness

Specimens of AA6061 alloy as-cast condition, AA6061- 5, 10, 15% as-cast condition and aged environments (AA6061 alloy was not aged) altogether. Seven samples of the composite were prepared to undergo the hardness tests. Vickers hardness experiments were executed before heat treatment at a constant load of 200gf, at room temperature. Fashion of enhancement of hardness value exhibited in AA6061-ZrO<sub>2</sub> 5%, AA6061-ZrO<sub>2</sub> 10% and AA6061-ZrO<sub>2</sub> 15% composite (as cast) specimen when compared to parent alloy is represented in figure 6(a). The improvement noticed was 12%, 24%, and 34% respectively.

As for aged composite specimen, an increment of hardness property was noticed in AA6061-ZrO<sub>2</sub> 5%, AA6061-ZrO<sub>2</sub> 10%, and AA6061-ZrO<sub>2</sub> 15%, and the same is represented in figure 6(b). The increment was 29%, 48%, and 72.3% respectively. The detailed increment in hardness of the cast and aged composite specimen is tabulated and presented in table 5. The cast composite specimen was quenched after solid solution treatment in order to sustain the composite rod in a supersaturated solid solution condition. Also during aging dissimilar needle/rod-shaped Mg-Si precipitates to have been formed within the AA6061 matrix. However, formed precipitates are micro sizes apparently visible in optical images as shown in figure 6. The enhancement of hardness was due to the character of precipitates, which was created at a particular time and diffusion of the ZrO<sub>2</sub> particles during the process of aging. The aging process would have been further promoted and accelerated the diffusion of Magnesium atoms; as a result, an excessive concentration of Magnesium was established in the complex oxides. From the above test and results, it has been proved that an increment of hardness value due to solid solution treatment and aging process. The proportions of magnesium and silicon available to form the magnesium silicide (Mg<sub>2</sub>Si) are predominant Magnesium and silicon are added either in balance amounts to form quasi-binary Al-Mg<sub>2</sub>Si alloys (Mg:Si 1.73:1), or with an excess of silicon above that needed to form Mg<sub>2</sub>Si. Independent clusters of Mg and Si atoms Co-clusters that contain Mg and Si atoms small precipitates of



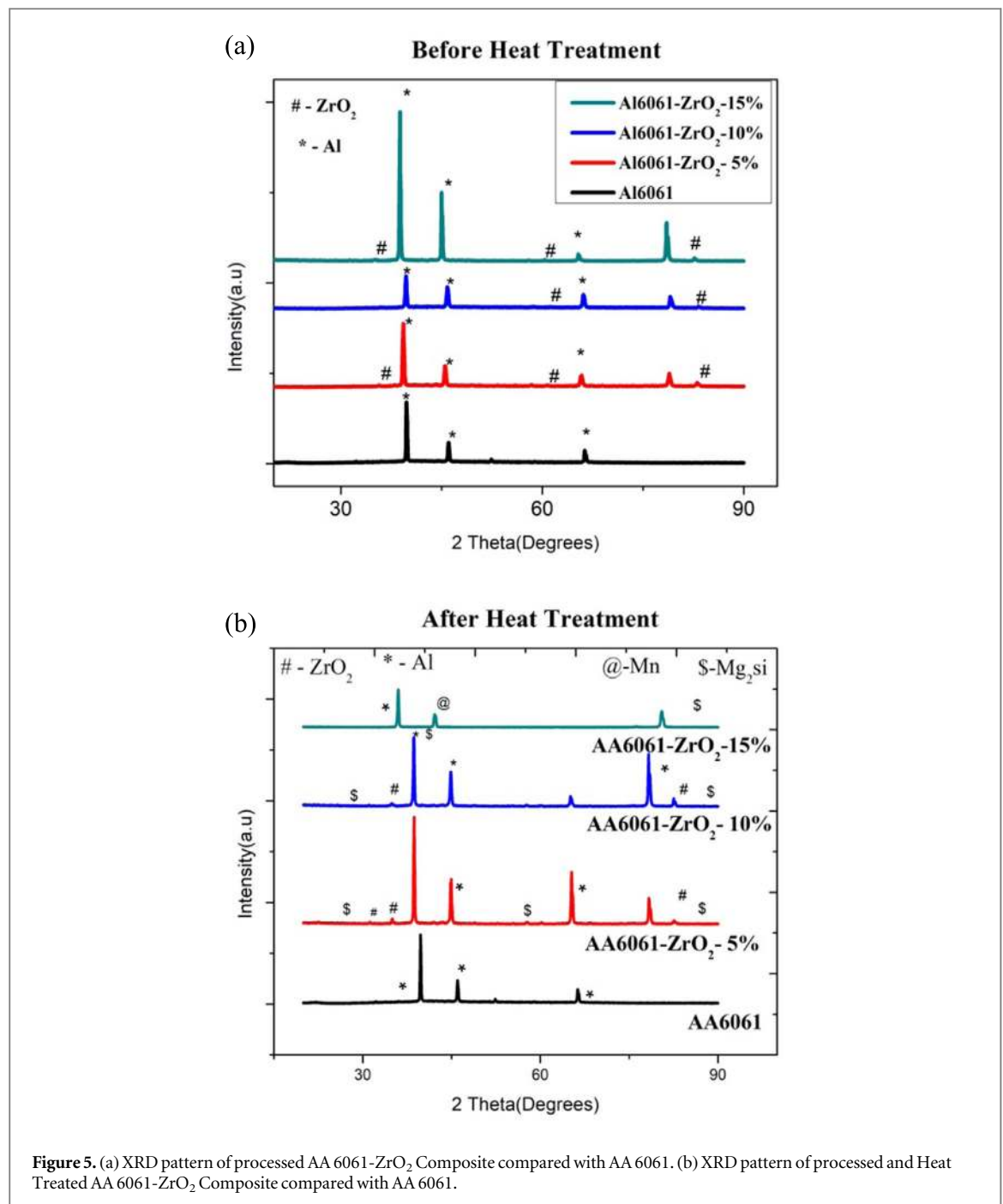
unknown structure  $\beta'$  needle-shaped precipitates of unknown structure B' Lath-shaped precipitates and  $\beta'$  rod-shaped precipitates.

Three types of clusters of atoms form in the early stage of aging of alloy 6061, clusters of Si atoms, clusters of Mg atoms and clusters that contain both Mg and Si atoms. It appears that independent clusters of Mg and Si atoms formed first, followed by the formation of Co-clusters. It is possible that both Mg-clusters of atoms and Si-clusters of atoms are formed immediately after quenching. Si atoms are thought to accompany vacancies when they condense, causing clustering to occur very soon after quenching.

The measure of the grain boundary of AA 6061 is diminished after the inclusion of fine ZrO<sub>2</sub> and squeeze casting. Application of outward pressure amid the solidification process builds the liquidus temperature of the alloy, which brings under cooling in the superheated alloy, bringing about better grain size. The microstructure of 6061 Al alloy was influenced by two primary components: inclusion of fine ZrO<sub>2</sub> and application of pressure amid the procedure of solidification of the melted as presented in figure 6.

### Impact of aging on tensile strength

The AA6061 alloy, cast composite, and aged composites were crafted into the tensile specimen and tested for tensile strength. The detailed increment in tensile value of the cast and aged composite specimen is tabulated and presented in table 6. The trend of tensile values demonstrates a 35% increase in tensile strength when the composite as-cast condition is evaluated against a parent AA6061 alloy. This attribute is obviously due to the insertion of hard reinforcement material particles, which have been already proved by many even though the reinforcement and values are not alike. Also, similar composites were developed with almost similar values of tensile strength but with different reinforcement with various percentage compositions [23–25]. Function of reinforcement particles is to give strength to the matrix. That's what happened in this process. G Gautam *et al*



concluded in their work that ultimate tensile strength of composites progressed considerably with 10 vol% Al<sub>3</sub>Zr particles but with an additional increase in the quantity of Al<sub>3</sub>Zr particles in the order 20%, 30%, these properties are undesirably reduced, nevertheless, hardness value continuously improved [26]. So it is expedient to limit the weight percentage to 15%. Additionally, the trend shows some interest due to the favoring dispersion of precipitates from the solid solution of AA6061 with respect to time. Highest tensile strength value was noticed for AA6061/ZrO<sub>2</sub>-15%. The percentage of the increase was about 63%. This was due to the higher or additional harmonized distribution of precipitates as a factor of temperature and time, indicated that the tensile value enhances in line with aging time at a uniform temperature of 205 °C. Furthermore, temperature and time influenced precipitation of a second phase the same paved the way to the enhancement of tensile strength [27–29]. Secondly, the solid solution AA6061-ZrO<sub>2</sub> particle's bond created in the interface enhanced tensile strength. It thirdly is due to the nucleation of precipitates bonding between AA6061 and ZrO<sub>2</sub> particles.

#### Mode of fracture observation of processed composite

Figures 7(a)–(d) demonstrates micrographs of the fractured specimens of parent alloy AA6061 and processed composite having 5, 10 and 15% reinforcement with the help of SEM. The mode of fracture of composites is

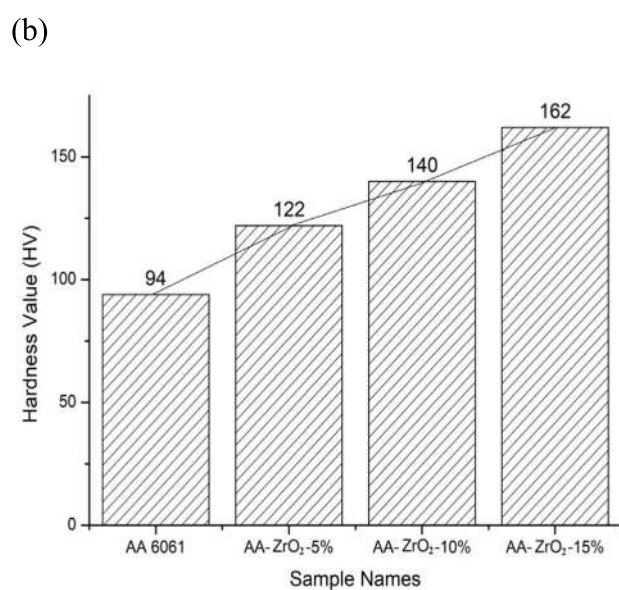
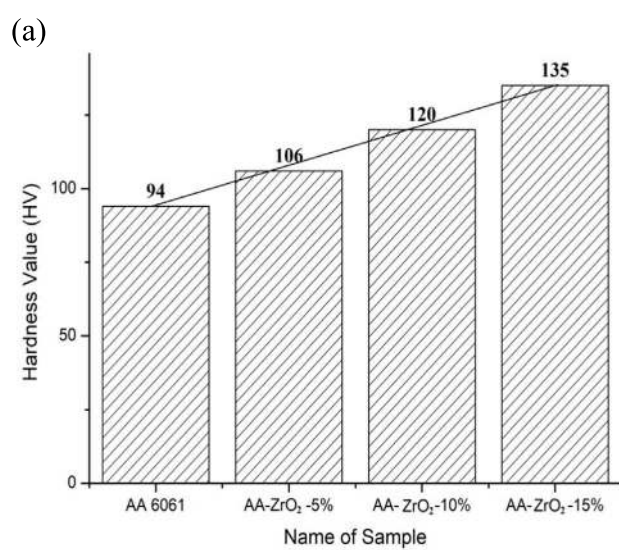
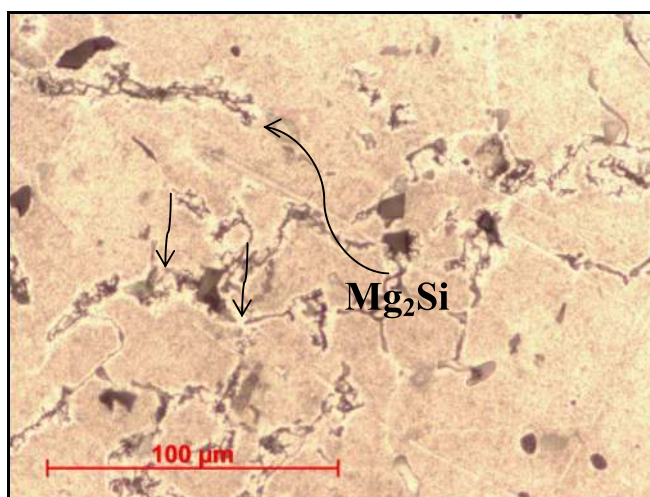


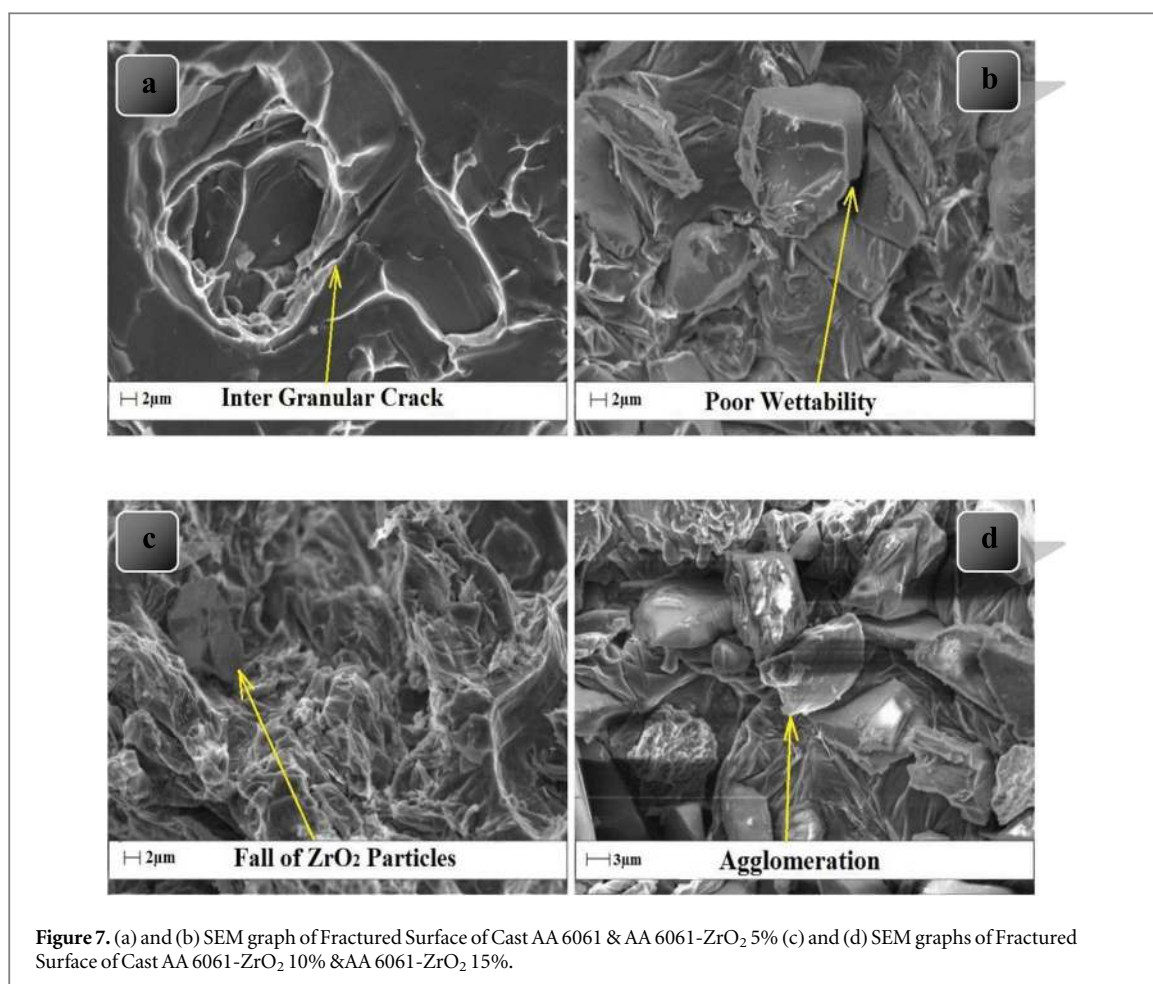
**Figure 6.** Mg<sub>2</sub>-Si precipitates in AA6061-ZrO<sub>2</sub> composites (aged). (a) Comparison of Hardness Value of AA 6061-ZrO<sub>2</sub> Composite (As Cast) with AA 6061 Parent Alloy. (b) Comparison of Hardness Value of AA 6061-ZrO<sub>2</sub> Composite (As Heat Treated) with AA 6061 Parent Alloy.

**Table 5.** Comparative chart to describe percentage increase of Micro hardness of cast composite.

Name of sample	Load (gf)	As cast - Hardness Value (HV)	% of Improvement	As heat treated-Hardness Value (HV)	% of Improvement
AA 6061	200	94			
Al-ZrO <sub>2</sub> -5%	200	106	12.8%	122	29.79%
Al-ZrO <sub>2</sub> -10%	200	120	24.5%	140	48.94%
Al-ZrO <sub>2</sub> -15%	200	135	34.2%	162	72.34%

**Table 6.** Comparative chart to describe percentage increase of UTS of cast composite.

Name of sample	As cast Ave. UTS (Mpa)	% of improvement	As heat treated Ave. UTS (Mpa)	% of Improvement
AA6061	92			
AA6061/ZrO <sub>2</sub> -5%	101	9.78	110	20
AA6061/ZrO <sub>2</sub> -10%	116	26.09	135	46
AA6061/ZrO <sub>2</sub> -15%	125	35.87	150	63



decided by quite a number of aspects like material and material fabrication parameters, which includes the type, size, shape, weight fraction, and dispersal of reinforcement elements in the matrix phase. Furthermore, mode of fracture depends upon matrix and interface property, such as precipitation effect, the interfacial bonding strength, porosity, etc. Many of these factors are mainly decided by synthesizing method and the procedures of heat treatment processes. The frequent causes of failure or breaking in particulate metal matrix composite are supposed to be the result of three dissimilar reasons. They are poor bonding, i.e. poor interfacial matrix-reinforcement, the breakage of particle reinforcement, and breakage or failure in the matrix itself. The fracture surface examinations demonstrate that the major prevailing fracture mechanism was the interdendritic cracking. During the solidification procedure of the composite, the alloy elements chiefly Si and ZrO<sub>2</sub> particles

**Table 7.** Represents the trend of wear of Processed AA 6061-ZrO<sub>2</sub> Composite. Reproduced with permission from [30]. [© Emerald Publishing Ltd, 2018.].

Sample Name	Load (N)	Speed (rpm)	Sliding distance in (mm)	Wear in (μm)
AA 6061 (A)	10	400	80	480
AA 6061 (B)	20	400	80	678
AA 6061 (C)	30	400	80	685
AA 6061-ZrO <sub>2</sub> 5% (D)	10	400	80	372
AA 6061-ZrO <sub>2</sub> 5% (E)	20	400	80	375
AA 6061-ZrO <sub>2</sub> 5% (F)	30	400	80	437
AA 6061-ZrO <sub>2</sub> 10% (G)	10	400	80	291
AA 6061-ZrO <sub>2</sub> 10% (H)	20	400	80	295
AA 6061-ZrO <sub>2</sub> 10% (I)	30	400	80	332
AA 6061-ZrO <sub>2</sub> 15% (J)	10	400	80	145
AA 6061-ZrO <sub>2</sub> 15% (K)	20	400	80	185
AA 6061-ZrO <sub>2</sub> 15% (L)	30	400	80	244

were rejected from the solid-liquid interface as a result these particles agglomerate or cluster at the interdendritic areas. Micro cracks spread beside the eutectic inter dendritic Al-Si and Si particle phase and show the way to breakage or failure of AA 6061 matrix. From this analysis, the predominant mode of failure of the composite is due to the breakage of AA6061 alloy. On the other hand, some regions of fractured regions of the composite specimens have dimples. This characteristic is due to the nucleation of cavities and their resulting amalgamation as an effect of huge shear deformations. Normally dimpled crack arises as a result of the introduction of voids at the eutectic Si particles.

### Wear property of processed AA 6061-ZrO<sub>2</sub> composite

Table 7 gives a representation of wear characteristic of prepared composite material for different load and percentage of composition of ZrO<sub>2</sub> in an arithmetical manner. The pin material is as cast AA 6061-ZrO<sub>2</sub> composite and the disc are made up of EN31 steel with hardness of 62 HRC. The test specimen, i.e. pin was curved as per ASTM: G99-05 standard. Tests were executed for four samples, and each sample consists of four samples, i.e. AA 6061 (Load 10, 20, 30N)—3 samples, AA 6061-ZrO<sub>2</sub> 5% (Load 10, 20, 30N)—3 samples, AA 6061-ZrO<sub>2</sub> 10% (Load 10, 20, 30N)—3 samples and AA 6061-ZrO<sub>2</sub> 15% (Load 10, 20, 30N)—3 samples all together 12 samples in as-cast conditions. As this composite material is exclusively designed for automotive component, preference was given to load. The other parameters are sliding velocity, which is 1.67 m s<sup>-1</sup> and sliding distance, which is 2000 m, which are kept constant during the entire experiment.

The variation in length of the pin was noted in microns and interpreted as wear resistance characteristic of AA 6061-ZrO<sub>2</sub> composite material. AA 6061-ZrO<sub>2</sub> 15% composite displays the lowest wear of 145 μm at 10N load when related to other samples. Subsequent lowest wear was noted by AA 6061-ZrO<sub>2</sub> 15% composite material at 20N load. This attribute is on account of the unique property of ZrO<sub>2</sub> elements realized in 15% composite. Figure 8 describes the trend of wear of prepared composite associated with the percentage of composition of ZrO<sub>2</sub> and load in a numerical way. This direct wear investigation data substantiates that the prepared composite owns enhanced wear a resistant characteristics than the base parent alloy AA 6061. Moreover, figure 8, undoubtedly, approves wear characteristic of the processed composite material is directly correlated to the applied load [31].

### Wear rate of processed AA 6061-ZrO<sub>2</sub> composite

Table 8 accounts the particulars of wear rate and wear resistance of established composite material in association to load and percentage of reinforcement particles. The formula needed to estimate specific wear rates are mentioned here.

$$\text{Wear rate} = \text{Volume loss in mm}^3 / \text{Sliding distance in meter}$$

$$\text{Wear resistance} = 1 / \text{Wear rate}$$

The lowest wear rate was offered by AA 6061-ZrO<sub>2</sub> 15% composite at 10N load, and the value is 0.0012 mm<sup>3</sup>/m, concurrently the same composite offered high wear resistance, and the value is 862 m/mm<sup>3</sup>. These experimental results prove that the increase of weight fractions of ZrO<sub>2</sub> can also incite clustering or agglomeration of the reinforcement particles during processing.

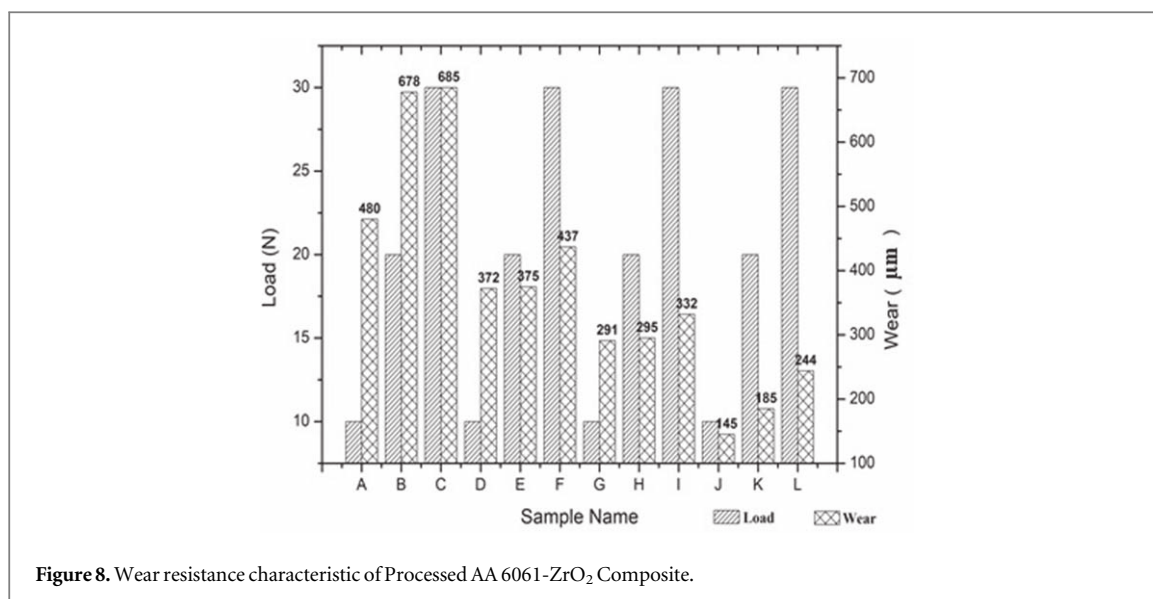


Figure 8. Wear resistance characteristic of Processed AA 6061-ZrO<sub>2</sub> Composite.

Well, bonding of the matrix phase with the particle phase increases wear resistance property of composite continuously with an escalation in the wt. percent of reinforcement material.

However, when the reinforcement particle phase was not appropriately bonded with the matrix phase, the wear-resistant property of the composite material increased up to a certain level of the reinforcement particle and afterwards started declining [32] (Hamid *et al* 2008).

#### Worn surface morphology of pin surface

Figures 9(a) and (b) shows the SEM images of the worn surface of AA 6061 at 30N load and AA 6061/ZrO<sub>2</sub> - 15% Composite at 30N. Study of worn surfaces at different parameters will give a clear picture of wear mechanism. Deep ploughing grooves, pit and gouge in alloy have been noticed in figure 9(a) especially on AA 6061-30N. This aspect depicts the reaction of aluminum when the huge amount of heat is caused due to the frictional force at high load and velocity.

Worn Surface Morphology of Processed AA 6061-ZrO<sub>2</sub> 15% confirms smooth and mild wear with wear debris on the surface as shown in figure 9(b). This is an attribute is of the fact that hard ZrO<sub>2</sub> particles prevented the formation of Deep ploughing grooves, pit and gouge.

#### Analysis of coefficient of friction (CoF) of prepared AA 6061-ZrO<sub>2</sub> composite

Table 9 describes the change of a coefficient of friction and frictional force with respect to load and percentage of reinforcements. CoF value decreases when the load increases, however, CoF value slightly increases when the percentage of reinforcement varies from 5% to 10% and remains the same at 15 wt%. The same trend was observed for Al<sub>3</sub>Zr composite the same was reported by (Gautam *et al* 2016) [26]. CoF is average when the steel disc rubs with AA 6061 at 10N, which is equal to 0.26.

When Steel surface was brought into contact with an AA 6061-ZrO<sub>2</sub> composite surface, the interfacial adhesive bonds that occurred in the actual area of contact were considerably strong that sharing or tearing formed locally in the AA 6061 matrix. As a result, the wear debris particles of AA 6061 were transferred to the steel surface during sliding. The coefficient of friction value increases as the entire surface energy of the metal increases.

#### Conclusions

From the study, the below conclusions have been drawn

- Materials for composite processing were chosen prudently and lucratively processed using stir casting attached with squeeze casting setup.
- EDX method emphasized the availability of desirable elements like aluminum, Zirconium, Oxygen and other elements like Mg, Si, Cr, etc.

**Table 8.** Calculated Values of Wear Rate and Wear Resistance of Processed AA 6061-ZrO<sub>2</sub>. Reproduced with permission from [30]. [© Emerald Publishing Ltd, 2018.].

Specimen name	Vol. loss in mm <sup>3</sup>	Wear rate value (mm <sup>3</sup> m <sup>-1</sup> )	Wear resistance value (m mm <sup>-3</sup> )	Specific wear rate value (mm <sup>3</sup> /Nm)
AA 6061-10N (A)	7.68	0.0038	260.417	0.0001
AA 6061-20N (B)	10.848	0.0054	184.366	0.0002
AA 6061-30N (C)	10.96	0.0055	182.482	0.0002
AA 6061-ZrO <sub>2</sub> 5% 10N (D)	5.952	0.0030	336.022	0.0001
AA 6061-ZrO <sub>2</sub> 5% 20N (E)	6	0.0030	333.333	0.0002
AA 6061-ZrO <sub>2</sub> 5% 30N (F)	6.992	0.0035	286.041	0.0002
AA 6061-ZrO <sub>2</sub> 10% 10N (G)	4.656	0.0023	429.553	0.0001
AA 6061-ZrO <sub>2</sub> 10% 20N (H)	4.72	0.0024	423.729	0.0002
AA 6061-ZrO <sub>2</sub> 10% 30N (I)	5.312	0.0027	376.506	0.0001
AA 6061-ZrO <sub>2</sub> 15% 10N (J)	2.32	0.0012	862.069	0.0001
AA 6061-ZrO <sub>2</sub> 15% 20N (K)	2.96	0.0015	675.676	0.0001
AA 6061-ZrO <sub>2</sub> 15% 30N (L)	3.904	0.0020	512.295	0.0002

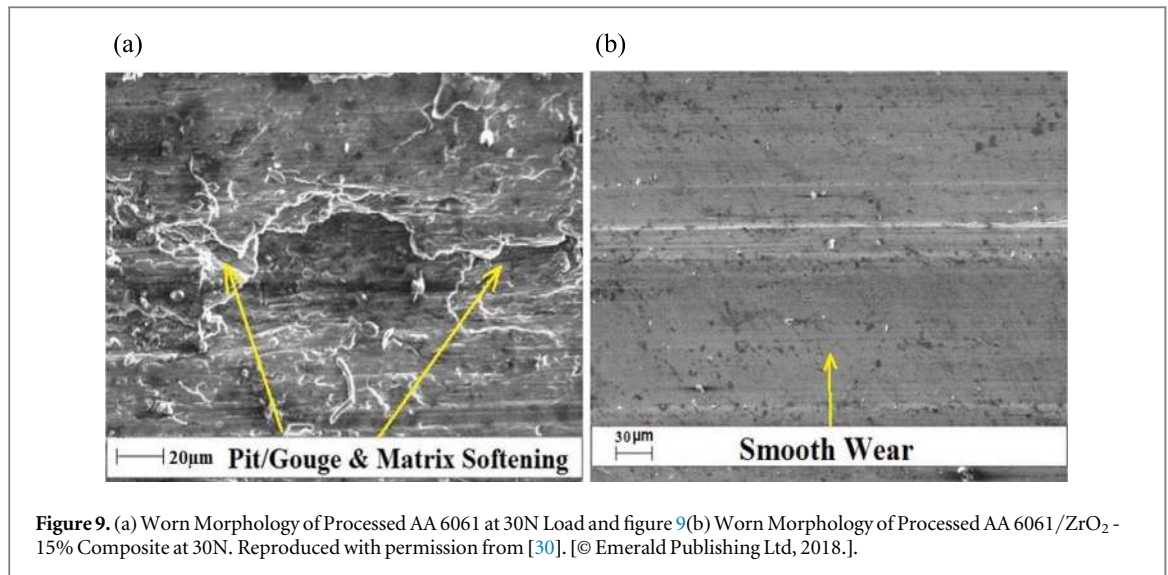


**Figure 9.** (a) Worn Morphology of Processed AA 6061 at 30N Load and figure 9(b) Worn Morphology of Processed AA 6061/ZrO<sub>2</sub>-15% Composite at 30N. Reproduced with permission from [30]. [© Emerald Publishing Ltd, 2018.]

**Table 9.** Experimental Values of Frictional Force and CoF of Processed AA 6061-ZrO<sub>2</sub> Composite. Reproduced with permission from [30]. [© Emerald Publishing Ltd, 2018.]

Sample	Load (N)	Speed (rpm)	Sliding distance (mm)	Frictional force (N)	CoF of Friction
AA 6061 (A)	10	400	80	7.5	0.26
AA 6061 (B)	20	400	80	9.5	0.33
AA 6061 (C)	30	400	80	9.5	0.32
AA 6061-ZrO <sub>2</sub> 5% (D)	10	400	80	6.5	0.35
AA 6061-ZrO <sub>2</sub> 5% (E)	20	400	80	7.2	0.36
AA 6061-ZrO <sub>2</sub> 5% (F)	30	400	80	5.1	0.26
AA 6061-ZrO <sub>2</sub> 10% (G)	10	400	80	6.2	0.33
AA 6061-ZrO <sub>2</sub> 10% (H)	20	400	80	3.1	0.32
AA 6061-ZrO <sub>2</sub> 10% (I)	30	400	80	9.5	0.31
AA 6061-ZrO <sub>2</sub> 15% (J)	10	400	80	4.2	0.39
AA 6061-ZrO <sub>2</sub> 15% (K)	20	400	80	3.8	0.37
AA 6061-ZrO <sub>2</sub> 15% (L)	30	400	80	3.2	0.29

- XRD graphs proves the presence of ZrO<sub>2</sub> and Mg<sub>2</sub>Si the compounds which paved the way for enhancement of hardness and strength in the processed AA-ZrO<sub>2</sub> composite
- The maximum hardness measurement was attained for AA-ZrO<sub>2</sub>-15% composite at 200gf, and the numerical value is 135 HV. And the highest tensile value was obtained for Al-ZrO<sub>2</sub>-15% composite, and the value is 125 MPa. This trait is due to the ZrO<sub>2</sub> particles, which give strength to the AA6061 matrix.
- Hardness property of heat treated AA 6061-ZrO<sub>2</sub> composite increased when compared with AA 6061 alloy (as cast) and the enhancement percentage was from 29%–72%. Tensile property of heat treated AA 6061-ZrO<sub>2</sub> composite increased when compared with AA 6061 alloy (as cast) and the enhancement percentage was from 20%–63%.
- The Fractography investigation depicts that failure was initiated by interdendritic cracking of the AA6061 matrix and fall of ZrO<sub>2</sub> particles from the clutches of matrix material which was seen with the help of SEM images.
- Wear studies were carried out upon the processed AA 6061-ZrO<sub>2</sub> composite and enhancement of wear resistance characteristic was evaluated. The wear resistance characteristic of AA 6061-ZrO<sub>2</sub> 15% composite at 30N load enhanced 1.5 times when compared to the AA 6061 parent alloy. Worn morphology study gives a picture of the type of wear, and a mild wear was observed due to the brittle reinforcement ZrO<sub>2</sub> particles. Also CoF value to some extent increases when the percentage of reinforcement varies from 5% to 10% and remains the identical at 15 wt%.
- This experimental result proposes a lightweight material to the manufacturing sector with enhanced strength having appreciable wear resistant property.

## Acknowledgments

The authors thank Dr Balan, School of Mechanical Engineering, VIT Vellore and Dr Muthuchamy, School of Mechanical Engineering, VIT Vellore for their useful technical inputs to accomplish this investigation work.

## ORCID iDs

Johny James  <https://orcid.org/0000-0002-7845-6927>

Chun-Ping Jen  <https://orcid.org/0000-0001-5558-5817>

## References

- [1] Mazahery A and Shabani M O 2012 Characterization of cast A356 alloy reinforced with nano SiC composites *Transactions of Nonferrous Metals Society of China* **22** 275–80.
- [2] Shabani M O and Mazahery A 2012 The performance of various artificial neurons interconnections in the modelling and experimental manufacturing of the composites *Materiali in Tehnologije* **46** 109–13
- [3] Kawabe A, Oshida A, Kobayashi T and Toda H 1999 Fabrication process of metal matrix composite with nano-size SiC particle produced by vortex method *Keikin-zoku/Journal of Japan Institute of Light Metals* **49** 149–54
- [4] Ramesh C S, Keshavamurthy R, Channabasappa B H and Ahmed A 2009 Microstructure and mechanical properties of Ni–P coated Si<sub>3</sub>N<sub>4</sub> reinforced Al6061 composites *Materials Science and Engineering: A* **502** 99–106
- [5] Bains P S, Sidhu S S and Payal H S 2016 Fabrication and machining of metal matrix composites: a review *Mater. Manuf. Processes* **31** 553–73
- [6] Kanta Das D, Mishra P C, Singh S and Thakur R K 2015 Tool wear in turning ceramic reinforced aluminum matrix composites—A review *J. Compos. Mater.* **49** 2949–61
- [7] Tun K S and Gupta M 2007 Improving mechanical properties of magnesium using nano-yttria reinforcement and microwave assisted powder metallurgy method *Compos. Sci. Technol.* **67** 2657–64
- [8] Gnanavelbabu A, Rajkumar K and Saravanan P 2018 Investigation on the cutting quality characteristics of abrasive water jet machining of AA6061-B4C-hBN hybrid metal matrix composites *Mater. Manuf. Processes* **33** 1313–23
- [9] Singh J and Chauhan A 2019 A review of microstructure, mechanical properties and wear behavior of hybrid aluminium matrix composites fabricated via stir casting route *Sādhanā*. **44** 16
- [10] Fairouz F M, Daoud A A and El-khair M T A Aging behavior and tensile properties of cast and squeezed 6061-SiC particles composites *21st Int. Conf. on Composite Materials Xi'an (20-25th August 2017)*
- [11] Kannan C, Ramamujam R and Balan A 2018 Machinability studies on Al7075/BN/Al<sub>2</sub>O<sub>3</sub> squeeze cast hybrid nanocomposite under different machining environments *Mater. Manuf. Processes* **33** 587–95
- [12] Lashgari H R, Sufizadeh A R and Emamy M 2010 The effect of strontium on the microstructure and wear properties of A356–10% B4C cast composites *Mater. Des.* **31** 2187–95
- [13] Saravanan V, Thyla P R and Balakrishnan S R 2016 A low cost, light weight cenosphere–aluminium composite for brake disc application *Bull. Mater. Sci.* **39** 299–305
- [14] Suthar J and Patel K M 2018 Processing issues, machining, and applications of aluminum metal matrix composites *Mater. Manuf. Processes* **33** 499–527
- [15] Kalaiselvan K, Murugan N and Parameswaran S 2011 Production and characterization of AA6061–B4C stir cast composite *Mater. Des.* **32** 4004–9
- [16] Li B, Luo B, He K, Zeng L, Fan W and Bai Z 2015 Effect of aging on interface characteristics of Al–Mg–Si/SiC composites *J. Alloys Compd.* **649** 495–9
- [17] Chen C L and Lin C H 2017 A study on the aging behavior of Al6061 composites reinforced with Y<sub>2</sub>O<sub>3</sub> and TiC *Metals* **7** 11
- [18] Karthikeyan G and Jinu G 2016 Dry sliding wear behavior optimization of stir cast LM6/ZrO<sub>2</sub> composites by response surface methodology analysis *Transactions of the Canadian Society for Mechanical Engineering* **40** 351–69
- [19] Kumar T S, Subramanian R, Shalini S and Angelo P 2016 Age hardening behaviour of Al–Si–Mg alloy matrix/Zircon and Alumina hybrid composite *J. Sci. Ind. Res.* **75** 89–94 <http://nopr.niscair.res.in/handle/123456789/33730>
- [20] Pradhan S, Ghosh S, Barman T K and Sahoo P 2017 Tribological behavior of Al–SiC metal matrix composite under dry, aqueous and alkaline medium *Silicon* **9** 923–31
- [21] Mahamani A and Anantha Chakravarthy V V 2017 Investigation on laser drilling of AA6061–TiB<sub>2</sub>/ZrB<sub>2</sub> *in situ* composites *Mater. Manuf. Processes* **32** 1700–6
- [22] Hashim J, Looney L and Hashmi M S J 2001 The enhancement of wettability of SiC particles in cast aluminium matrix composites *J. Mater. Process. Technol.* **119** 329–35
- [23] Sun C, Song M, Wang Z and He Y 2011 Effect of particle size on the microstructures and mechanical properties of SiC-reinforced pure aluminum composites *J. Mater. Eng. Perform.* **20** 1606–12
- [24] Amir Khanlou S and Niroumand B 2011 Development of Al356/SiCp cast composites by injection of SiCp containing composite powders *Mater. Des.* **32** 1895–902
- [25] Mazaheri Y, Meratian M, Emadi R and Najarian A R 2013 Comparison of microstructural and mechanical properties of Al–TiC, Al–B4C and Al–TiC–B<sub>4</sub>C composites prepared by casting techniques *Materials Science and Engineering: A* **560** 278–87
- [26] Gautam G, Kumar N, Mohan A, Gautam R K and Mohan S 2016 Synthesis and characterization of tri-aluminide *in situ* composites *J. Mater. Sci.* **51** 8055–74
- [27] Sharma A, Sharma V M, Mewar S, Pal S K and Paul J 2018 Friction stir processing of Al6061–SiC-graphite hybrid surface composites *Mater. Manuf. Processes* **19** 33 795–804
- [28] Hassan S B, Aponbiede O and Aigbodion V S 2008 Precipitation hardening characteristics of Al–Si–Fe/SiC particulate composites *J. Alloys Compd.* **466** 268–72
- [29] Ithom A P, Bem N G, Anbua E E and Ogbodo J N 2012 The effect of ageing time on some mechanical properties of Aluminum/0.5% glass reinforced particulate composite *Journal of Minerals and Materials Characterization and Engineering* **11** 919

- [30] James J and Raja Annamalai A 2018 Tribological Behaviour and Wear Fashion of Processed AA6061/ZrO<sub>2</sub> Composite *Ind. Lubr. Tribol.* **70** 1815–24
- [31] Rao R and Das S 2011 Effect of sic content and sliding speed on the wear behaviour of aluminium matrix composites *Mater. Des.* **32** 1066–71
- [32] Hamid A A, Ghosh P, Jain S and Ray S 2008 The influence of porosity and particles content on dry sliding wear of cast *in situ* Al (Ti)–Al<sub>2</sub>O<sub>3</sub> (TiO<sub>2</sub>) composite *Wear* **265** 14–26